

Self-Assembled Bolaamphiphile Fibers Have Intermediate Properties between Crystalline Nanofibers and Wormlike Micelles: Formation of Viscoelastic Hydrogels Switchable by Changes in pH and Salinity

Gesche Graf,[†] Simon Drescher,^{†,‡} Annette Meister,^{†,§} Bodo Dobner,[‡] and Alfred Blume^{*,†}

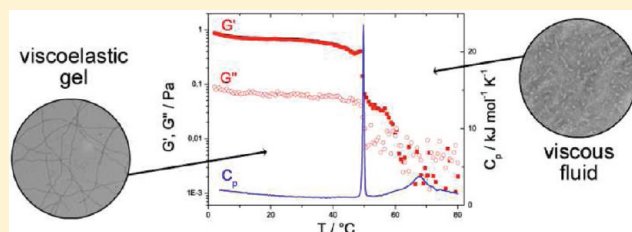
[†]Physical Chemistry, Institute of Chemistry, Martin-Luther-University Halle-Wittenberg, Von-Danckelmann-Platz 4, 06120 Halle, Germany

[‡]Biochemical Pharmacy, Institute of Pharmacy, Martin-Luther-University Halle-Wittenberg, Wolfgang-Langenbeck-Strasse 4, 06120 Halle, Germany

[§]ZIK HALOmem, Martin-Luther-University Halle-Wittenberg, Kurt-Mothes-Strasse 3, 06120 Halle, Germany

 Supporting Information

ABSTRACT: The aggregation behavior and rheological properties of aqueous suspensions of the bolaamphiphile dotriacontane-1,32-diyl-bis[2-(dimethylammonio)ethylphosphate] ($\text{Me}_2\text{PE-C32-Me}_2\text{PE}$) were investigated depending on the pH value and the salinity by means of differential scanning calorimetry (DSC), transmission electron microscopy (TEM), and oscillatory rheology. This bolaamphiphile self-assembles into helical fibers of approximately 5 nm thickness with an all-*trans* conformation of the alkyl chains. These nanofibers can gel water very effectively by forming a three-dimensional network. The headgroups' protonation depends on the pH value of the solution and influences the ability of the molecules to aggregate into fibers. At low pH values the headgroups are zwitterionic and stable hydrogels are formed, whereas at high pH values the headgroups are negatively charged and the length of the fiber aggregates diminishes as does the stability of the gel structure. We can show that by the addition of cations it is possible to shield the repulsive interaction between the molecules at high pH values so that the formation of the fiber aggregates and the gelation of the system occur. By addition of salt at high pH values the viscous flow behavior of $\text{Me}_2\text{PE-C32-Me}_2\text{PE}$ suspensions could be transformed into the viscoelastic behavior of a gel. The gels show characteristics that are common in systems of wormlike micelles. However, there are also significant differences that arise from the unique bolaamphiphile fiber structure with highly ordered alkyl chains that render the properties similar to crystalline nanofibers.



INTRODUCTION

Gels formed by crystalline nanofibers or wormlike micelles in water are a field of research that has gained much interest due to the large variety of substances that can be utilized for different possible applications such as sensors or optical components,¹ tissue engineering,² or drug release and delivery.³ Organic gelators can on the one hand consist of large threadlike molecules such as biological macromolecules (e.g., gelatin, actin, or collagen) or block copolymers. On the other hand, low molecular weight gelators are especially interesting as they first have to self-assemble into larger aggregates that subsequently gel the solvent by interactions between the aggregates (e.g., hydrogen bonds, hydrophobic interaction, or simply entanglements).^{2,4} Therefore, they are also interesting for biological applications as they are easier to degrade than most polymers.³ In the case of low molecular weight gelators it is easy to influence the gelling properties of the substances by changing parameters such as the temperature, pH value, or salinity to achieve well-defined properties.^{5–7} The small-molecule gelators are mostly amphiphiles,

i.e., they contain a hydrophobic and a hydrophilic part, such as surfactants^{4,8} or lipids.⁹ Another possibility are sugar-based systems.² One special class of lipids are the so-called bolaamphiphiles or bolalipids consisting of a hydrophobic spacer (e.g., one or two alkyl chains) connected to hydrophilic groups (e.g., sugars or phosphocholine) at both ends.¹⁰ They can self-assemble to form a variety of aggregates such as monolayer membranes, nanotubes, or nanofibers.¹¹ These nanofibers have been shown to build stable and transparent hydrogels.⁷

We have recently reported on the aggregation behavior of symmetrical single-chain bolaamphiphiles consisting of one very long alkyl chain and two phosphocholine (PC-*C_n*-PC) or two phosphodimethylethanolamine ($\text{Me}_2\text{PE-C_n$ - Me_2PE) headgroups with $n = 22–36$ (Figure 1).^{12–16} Other functionalities of the headgroups were also introduced, e.g., amino groups¹⁷ or

Received: June 9, 2011

Revised: July 14, 2011

Published: July 14, 2011

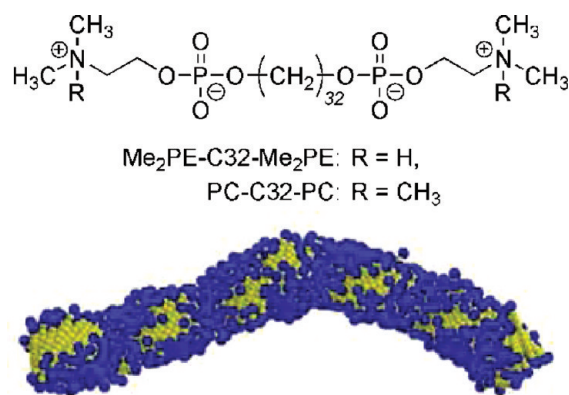


Figure 1. (top) Chemical structure of the bolalipids $\text{Me}_2\text{PE-C32-Me}_2\text{PE}$ ($\text{R} = \text{H}$) and PC-C32-PC ($\text{R} = \text{CH}_3$) and (bottom) coarse-grained off-lattice Monte Carlo simulation of the fiber structure formed in aqueous suspension.

sulfur-containing moieties.¹⁸ These bolaamphiphiles self-assemble in water into helical fibers (Figure 1) and micelles depending on the concentration, temperature, and pH value of the suspension.¹⁹ In the case of PC headgroups the self-assembly process is exclusively driven by hydrophobic interactions between the all-*trans* alkyl chains. In contrast, the Me_2PE headgroups can form additional hydrogen bonds leading to increased stability of the fibers at high temperatures. The self-assembled nanofibers are able to form a three-dimensional network that leads to the complete gelation of the aqueous system. The viscoelastic gel structure is on the one hand stabilized by cross-linking of the fibers supported by interactions between the hydrophobic parts at the fiber surface that are exposed to the water. On the other hand, in the case of zwitterionic Me_2PE headgroups at pH 5, additional stabilization occurs via hydrogen bonds between the headgroups of different fiber strands.

For $\text{Me}_2\text{PE-C32-Me}_2\text{PE}$ the formation of fibers depends on the pH value of the suspension. At neutral pH values the bolalipid has a zwitterionic headgroup (Figure 1). The apparent pK_a values for the phosphate group and the dimethylammonium group were determined to be approximately 3.3 and above 7, respectively.¹⁵ Therefore, at high pH values the headgroup is deprotonated and negatively charged and the aggregation into fibers becomes unfavorable due to the repulsion between the negatively charged molecules. However, small-angle neutron scattering (SANS) and transmission electron microscopic (TEM) measurements still prove the presence of short fiber segments, but no gelation of the system can be observed.^{15,19} This suggests that the charged headgroups mainly prevent the entanglements and interactions stabilizing the gel structure, regardless that the formation of shorter fibers is still possible.

The aggregates can be described as nanofibers, but they are more like an intermediate state between classical crystalline nanofibers and wormlike micelles of surfactants as they have properties similar to both systems.^{4,9} In contrast to classical crystalline fibers they form clear homogeneous gels that have quite high straining limits (see rheological data) and the SANS data show a slope of -1 in a plot of intensity I versus wave vector q .¹⁹ On the other hand, disrupted gels of the symmetrical single chain bolaamphiphiles take several hours to recover, a behavior which is uncommon in systems of wormlike surfactant gels.⁹

The aim of this study was to investigate how the aggregation behavior of $\text{Me}_2\text{PE-C32-Me}_2\text{PE}$ can be influenced to obtain

fibers and viscoelastic gels, tailoring the properties via changes of pH value and salt contents. Changing the pH value is a suitable way of adjusting the protonation in different parts of the molecules and thus controlling the self-assembly. In combination, the shielding of repulsive interaction between charged headgroups by means of additional salts is a promising method. This has already been tried with a bolalipid containing positively charged amino moieties in the headgroups.¹⁷ The stabilizing effect of salts on different aggregates has been often described, e.g., for collagen fibers,²⁰ for the rheological properties of mixtures of gellan gum and konjac glucomannan,²¹ for interactions between phospholipids and calcium,²² or for cationic wormlike micelles.²³

EXPERIMENTAL METHODS

Dotriacontane-1,32-diyl-bis[2-(dimethylammonio)ethylphosphate] ($\text{Me}_2\text{PE-C32-Me}_2\text{PE}$) was synthesized as described recently.^{12,13} The suspensions of the bolalipids were prepared with ultrapure water from a Milli-Q A10 system (Millipore GmbH, Schwalbach, Germany). Salts were purchased from Carl Roth GmbH & Co. (Karlsruhe, Germany) and were used without further purification.

Sample Preparation. The appropriate amount of bolalipid was suspended in water or buffer (pH 5, 10 mM acetate buffer). For the measurements at pH 11 with different salts, the pH value was adjusted with very small amounts of a 2.5 M NaOH solution after degassing the samples for 15 min. To achieve a homogeneous suspension, the samples were heated above 70 °C three times and vortexed.

Differential Scanning Calorimetry (DSC) Measurements. The DSC measurements were made with a Microcal VP-DSC (MicroCal Inc., Northampton, MA, USA). The concentration of the bolalipid suspensions was 1 mg mL⁻¹; water or buffer was used as reference. For the salt-containing samples, the suspensions were prepared in an aqueous salt solution of the required concentration. The samples were degassed prior to adjustment of the pH value. Measurements were carried out with a heating rate of 20 °C h⁻¹ in the temperature interval from 2 to 95 °C. To check reproducibility, three consecutive scans of each sample were recorded.

Rheology. The rheological measurements were carried out with an Anton Paar MCR 301 rheometer (Anton Paar GmbH, Graz, Austria) controlled by the software RheoPlus 3.0. For the oscillatory measurements we used a cone-plate shear system (2°, 50 mm) with a thermostating unit (Peltier system; -40 to 200 °C) and a thermostatted hood to improve temperature stability. The bolalipid suspensions used had a concentration of 1 mg mL⁻¹. The sample was left to equilibrate for 30 min at 2 °C before the start of the heating and cooling cycle with a heating rate of 20 °C h⁻¹. To prevent the evaporation of water, the cone and gap were covered with small amounts of low viscosity silicone oil.

Transmission Electron Microscopy (TEM). TEM images were recorded with a Zeiss EM 900 transmission electron microscope (Carl Zeiss NTS GmbH, Oberkochen, Germany). Five microliters of the sample solution was spread on a copper grid coated with a Formvar film. After 1 min the excess solution was blotted off with filter paper. The samples were stained with 1% uranyl acetate solution (20 μL) which was drained off after 1 min. The samples were dried at 30 °C overnight. For the samples prepared below ambient temperature, the components were stored (24 h) and

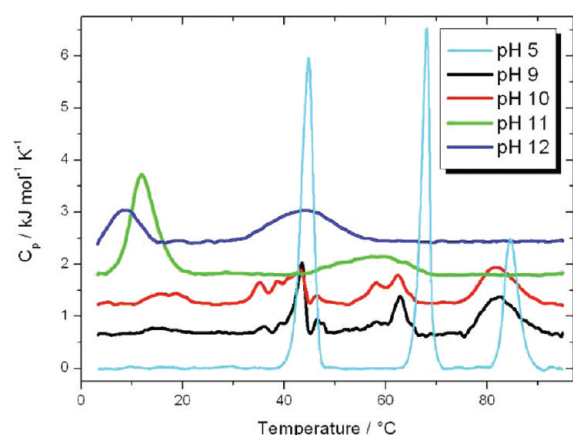


Figure 2. DSC heating curves of aqueous suspensions ($c = 1 \text{ mg mL}^{-1}$) of $\text{Me}_2\text{PE-C32-Me}_2\text{PE}$ in buffer at pH 5 and at pH values from 9 to 12 (adjusted with NaOH solution). The heating rate was $20 \text{ }^\circ\text{C h}^{-1}$. The DSC curves are shifted horizontally for clarity.

prepared in a cold room ($5 \text{ }^\circ\text{C}$). They were dried for 2 days at $5 \text{ }^\circ\text{C}$ and kept in an exsiccator at ambient temperature until the images were recorded.

Dynamic Light Scattering (DLS). The DLS experiments were carried out with an ALV-NIBS-HPPS particle sizer (ALV-Laser Vertriebgesellschaft mbH, Langen, Germany). The device was equipped with a 3 mW HeNe laser with a wavelength of 632.8 nm, and a scattering angle of 173° was used. All samples ($c = 1 \text{ mg mL}^{-1}$) were filtered through a membrane filter of $0.45 \mu\text{m}$ pore size (at $80 \text{ }^\circ\text{C}$) into the cuvettes. Before starting the measurement, each sample was equilibrated for 30 min. Three individual measurements were performed for each system to test the reproducibility. The experimental data were analyzed with the aid of the ALV-5000/E software taking into account the temperature correction of the viscosity.

RESULTS AND DISCUSSION

pH Dependent Aggregation Behavior. To investigate the pH dependence of the aggregation behavior of $\text{Me}_2\text{PE-C32-Me}_2\text{PE}$ and possible influences of buffer salts, we performed a series of differential scanning calorimetry measurements (DSC) at different pH values to analyze the changes in transition temperatures (Figure 2). In acetate buffer at pH 5 we can observe three transitions as reported before, with the first being a fiber–fiber transition ($45 \text{ }^\circ\text{C}$), the second a fiber–micelle transition ($68.2 \text{ }^\circ\text{C}$), and the third a micelle–micelle transition ($84.5 \text{ }^\circ\text{C}$). These transformations between different aggregate structures have been studied before with several methods, e.g., TEM, SANS, and Fourier transform infrared (FT-IR) spectroscopy.^{15,19,24} The first transition is connected with an increase in *gauche* conformers of the alkyl chains as was determined by FT-IR measurements.¹⁵ However, the fiber structure is still intact, which is due to hydrogen bonding between the headgroups.

First rheological measurements showed that this transition is connected with a large drop in the elasticity of the gel structure,¹⁹ suggesting that the entanglement of the fibers is weakened. The second DSC peak was found to be connected with the transformation of the fibers into spherical micelles with a radius of 2.64 nm as determined by SANS measurements.¹⁹ The third transition is a micelle–micelle transition during which the

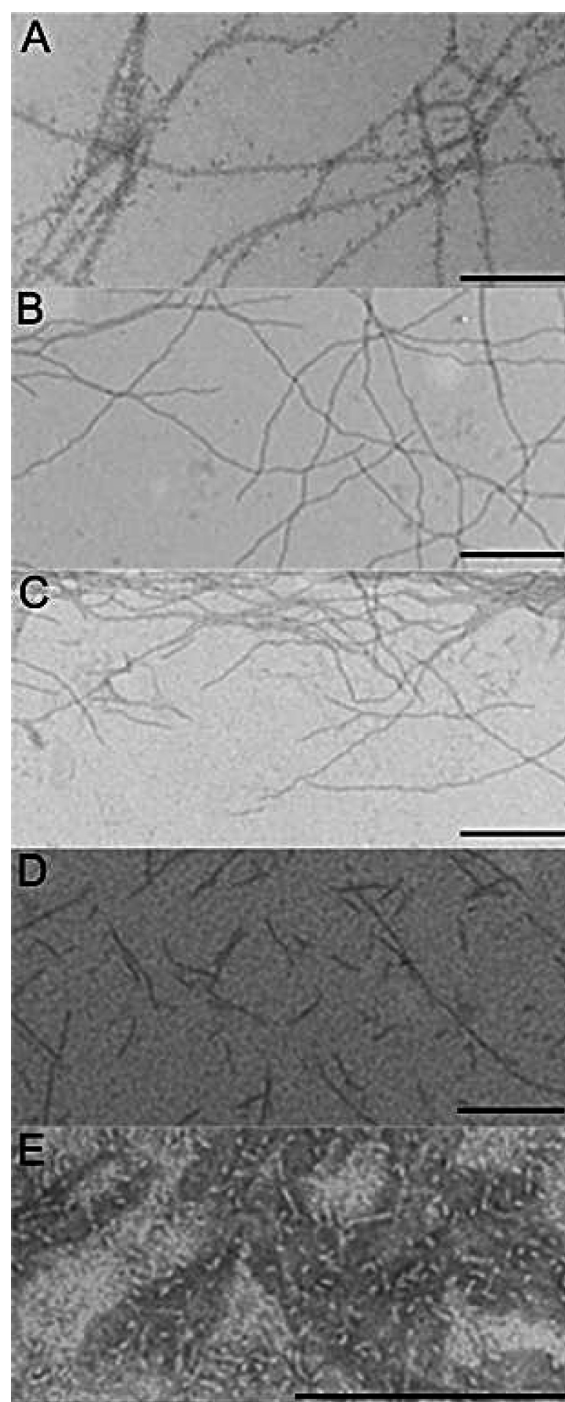


Figure 3. TEM images of aqueous suspensions of $\text{Me}_2\text{PE-C32-Me}_2\text{PE}$ at (A) pH 9 ($25 \text{ }^\circ\text{C}$), (B) pH 10 ($25 \text{ }^\circ\text{C}$), (C) pH 11 ($5 \text{ }^\circ\text{C}$), (D) pH 12 ($5 \text{ }^\circ\text{C}$), and (E) pH 11 ($25 \text{ }^\circ\text{C}$). The bar corresponds to 200 nm. The samples were stained with uranyl acetate.

amount of *gauche* conformers in the alkyl chain further increases, but where the structural differences between the two types of micelles are still unclear.

At pH 9 and 10, the first and second transitions appear very broad and divided into several small peaks, but there are still peaks left at the same temperatures that were observed at pH 5. The third transition is hardly influenced at these pH values. At pH 10 we can already observe a small transition below $20 \text{ }^\circ\text{C}$.

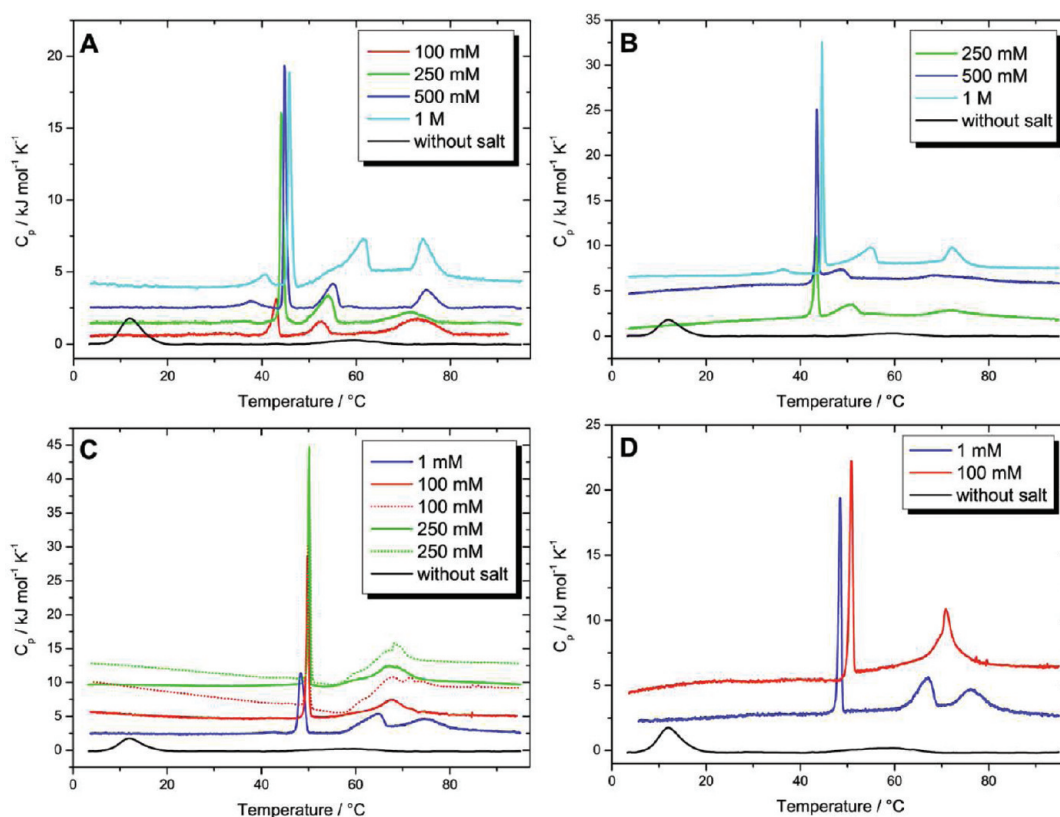


Figure 4. DSC heating curves of aqueous suspensions ($c = 1 \text{ mg mL}^{-1}$) of $\text{Me}_2\text{PE-C32-Me}_2\text{PE}$ at pH 11 with different concentrations of (A) NaCl, (B) KCl, (C) MgCl_2 , and (D) CaCl_2 . The heating rate was 20°C h^{-1} for the solid curves and 60°C h^{-1} for the dotted curves (C). The DSC curves are shifted horizontally for clarity.

A larger effect becomes visible at pH 11 as the DSC curve just shows two broad peaks around 12 and 60 $^\circ\text{C}$, respectively. This tendency increases at pH 12: then two broad transitions at 9 and 44 $^\circ\text{C}$ can be observed.

Transmission electron microscopy (TEM) images were taken to determine the aggregate structures at the different pH values (Figure 3). At 25 $^\circ\text{C}$ the suspensions at pH 9 and 10 show the presence of fibers (Figure 3A,B). The suspensions at pH 11 and 12 were prepared at 5 $^\circ\text{C}$, and these samples also show the aggregation into fibers below the first transition (Figure 3C,D). The presence of short fiber segments in the sample at pH 12 is due to the very low temperature of the transition starting at 2 $^\circ\text{C}$. If the suspensions are kept at 4 $^\circ\text{C}$ in the refrigerator for a few weeks, gelation can be observed for all pH values. The strongest gel seems to be formed at pH 9.

Using dynamic light scattering (DLS), we examined the aggregate structure in the suspensions at pH 11 and 12 at 30 $^\circ\text{C}$ above the first transition. The experiments reveal the presence of spherical micelles with a radius of 2.6 nm for both pH values (Figure S1 in the Supporting Information). This is also in accordance with the TEM image of a sample at pH 11 at 25 $^\circ\text{C}$ showing micelles (Figure 3E).

DSC and TEM prove that the fiber structure is destabilized at pH 9 and 10; the self-aggregation into fibers, however, is not completely inhibited at these pH values. The DSC curves reveal the presence of a mixture of aggregate types such as fibers, short fiber segments, and micelles as can be seen by the appearance of several small transition peaks. This was also observed in SANS measurements with the suspension in carbonate buffer at pH 10.¹⁹

The deprotonation of the dimethylammonium headgroup does not seem to be complete at pH 10, and the changes in aggregation behavior at increasing temperatures basically follow the same pattern as at pH 5. Probably, the fibers can tolerate a certain percentage of the negatively charged headgroups merely leading to reduced interactions between the fibers and to shorter fiber segments. However, a much larger shift of the transitions for samples at pH 11 and 12 to lower temperatures indicate that the effect of deprotonation with increasing negative charge of the headgroup is getting stronger and that the fibers are now only stable up to 12 or 9 $^\circ\text{C}$, respectively. These results suggest that the apparent pK_a value of the dimethylammonium group is between pH 10 and 11 in solutions with low ionic strength. The previously reported apparent pK_a value of 6.5 was obtained by using an automatic titrator with $\text{Me}_2\text{PE-C32-Me}_2\text{PE}$ dissolved in 150 mM KCl.¹⁵ As the apparent pK_a values depend on the ionic strength of a solution and are shifted to lower values with increasing salt concentration, it can be expected that the apparent pK_a value deduced from the DSC measurements without additional salts is higher than the previously determined one.

The fiber structure of $\text{Me}_2\text{PE-C32-Me}_2\text{PE}$ is stabilized on the one hand by hydrophobic interactions between the alkyl chains. On the other hand, $\text{Me}_2\text{PE-C32-Me}_2\text{PE}$ is able to form hydrogen bonds between its headgroups that further increase the stability of the aggregates and the gel structure. As the deprotonation of the Me_2PE headgroup increases with higher pH values, this additional attractive interaction is overcompensated by an increasing repulsive interaction due to the negative charge of the phosphate group. The stability range of the self-assembled

Table 1. DSC Transition Temperatures and Enthalpies of Aqueous Suspensions of Me₂PE-C32-Me₂PE at pH 11 with Different Concentrations of NaCl and KCl

	$T/^{\circ}\text{C}$ ($\Delta H/\text{kJ mol}^{-1}$) ^a						
	NaCl				KCl		
	100 mM	250 mM	500 mM	1 M	250 mM	500 mM	1 M
first transition	42.9 (4.8)	44.2 (12.8)	44.8 (12.2)	45.9 (12.8)	43.4 (8.2)	43.4 (10.8)	44.7 (12.7)
second transition	52.5 (2.7)	54.0 (7.3)	55.1 (4.9)	61.8 (8.1)	50.7 (4.4)	48.7 (2.3)	55.1 (6.5)
third transition	73.2 (8.2)	71.9 (4.9)	74.9 (5.0)	74.3 (7.1)	72.0 (4.7)	68.7 (5.7)	72.3 (5.2)

^a The transition temperatures and enthalpies were determined from the DSC heating curves ($c = 1 \text{ mg mL}^{-1}$) with a heating rate of $20^{\circ}\text{C h}^{-1}$.

nanofibers is therefore shifted to lower temperatures with increasing deprotonation of the dimethylammonium group.

Salt Dependent Aggregation Behavior at pH 11. We were further interested in the possibility of influencing the aggregation behavior of suspensions of Me₂PE-C32-Me₂PE in addition to changing the temperature or the pH value. The negative net charge of the headgroup at high pH clearly caused a destabilization of the fiber structure. The addition of salts seems to be a suitable way of shielding this charge and enabling the adjustment of specific aggregates depending on the pH value and the salinity.

To make sure that we worked with defined aggregates, we chose to use pH 11 for all suspensions as the previous results indicate that there are only micelles present at ambient temperature and no mixture of different aggregates such as micelles, short fiber segments, and nanofibers (Figure 3E).

In order to investigate the effect of different salts on the system, we performed DSC measurements with suspensions of Me₂PE-C32-Me₂PE at various concentrations of NaCl, KCl, MgCl₂, and CaCl₂ to compare the different monovalent and divalent cations while keeping the anions the same (Figure 4).

The DSC heating curves for NaCl concentrations from 100 mM to 1 M are shown in Figure 4A. It is obvious that the addition of NaCl causes a general increase in the transition temperatures. Even at low concentrations, the DSC curves reveal a profile comparable to that in acetate buffer at pH 5. With increasing concentrations the first transition is slightly shifted to higher temperatures, whereas the third transition becomes more cooperative with higher salt content. The largest effect of increasing salt concentration is observed for the second transition, where the temperature gradually increases from 52.5°C at 100 mM NaCl to 61.8°C at 1 M NaCl. At concentrations of 500 mM and 1 M NaCl a fourth transition appears at temperatures below the first one. This small transition was observed previously for the zwitterionic bolaamphiphile PC-C32-PC.¹⁴ The occurrence of this transition is dependent on the concentration of the bolalipid and the equilibration time before the measurement.¹⁴ The longer a sample is equilibrated or the higher the concentration, the more pronounced the transition becomes. The DSC measurements suggest that this small transition also correlates with the salt concentration. An overview of the transition temperatures and enthalpies determined by DSC is shown in Table 1.

The effect of KCl concentrations from 250 mM to 1 M on the Me₂PE-C32-Me₂PE suspensions at pH 11 can be seen in Figure 4B. Similarly as for solutions containing the sodium counterpart, the DSC heating curves exhibit three distinct peaks. With increasing KCl concentration the first transition is slightly shifted to higher temperatures and the third transition becomes

Table 2. DSC Transition Temperatures and Enthalpies of Aqueous Suspensions of Me₂PE-C32-Me₂PE at pH 11 with Different Concentrations of MgCl₂ and CaCl₂

	$T/^{\circ}\text{C}$ ($\Delta H/\text{kJ mol}^{-1}$) ^a				
	MgCl ₂			CaCl ₂	
	1 mM	100 mM	250 mM	1 mM	100 mM
first transition	48.3 (12.7)	49.8 (15.0)	50.1 (14.3)	48.4 (12.6)	50.9 (14.1)
second transition	64.8 (10.7)	67.6 (19.0)	68.0 (17.5)	67.0 (7.7)	70.8 (16.0)
third transition	74.6 (8.5)			75.9 (8.1)	

^a The transition temperatures and enthalpies were determined from the DSC heating curves ($c = 1 \text{ mg mL}^{-1}$) with a heating rate of $20^{\circ}\text{C h}^{-1}$.

more cooperative. Again, the second transition shows the strongest dependence on increasing concentration, with the second and third transitions for 500 mM KCl seeming to be an exception to this tendency (Table 1).

The binding of monovalent cations to negatively charged phosphate groups of phosphodiester is usually weak. This is different for the binding of divalent cations such as magnesium or calcium ions, as has been studied in detail for the binding to lipid vesicles containing dimyristoylphosphatidylglycerol.²⁹ For the binding to the negatively charged headgroups of Me₂PE-C32-Me₂PE, effects similar to those observed for the binding to the headgroup region of flat bilayers are to be expected.

The DSC curves for Me₂PE-C32-Me₂PE suspensions containing magnesium and calcium chlorides show significant differences as compared to suspensions containing monovalent ions. Even for low concentrations of 1 mM the aggregation behavior changes drastically. As can be seen in Figure 4C, the DSC curve at 1 mM MgCl₂ has three peaks at 48.3, 64.8, and 74.6°C , suggesting an aggregation behavior of the bolaamphiphile similar to that in acetate buffer (pH 5). When the concentration is further increased, only two transitions at 49.8 and 67.6°C appear. The second transition seems to be situated between the second and third transitions of the sample with 1 mM MgCl₂. Above the concentration of 250 mM MgCl₂ only a small further increase of the transition temperatures can be observed. Similar effects can be seen for measurements with CaCl₂ solutions (Figure 4D). However, suspensions with a concentration higher than 100 mM CaCl₂ could not be examined because of precipitation of aggregates. Detailed information on transition temperatures and enthalpies is provided in Table 2.

To identify the structure of the aggregates below the first transition, we recorded TEM images of the suspensions containing 100 mM NaCl and 250 mM MgCl₂, respectively. Samples

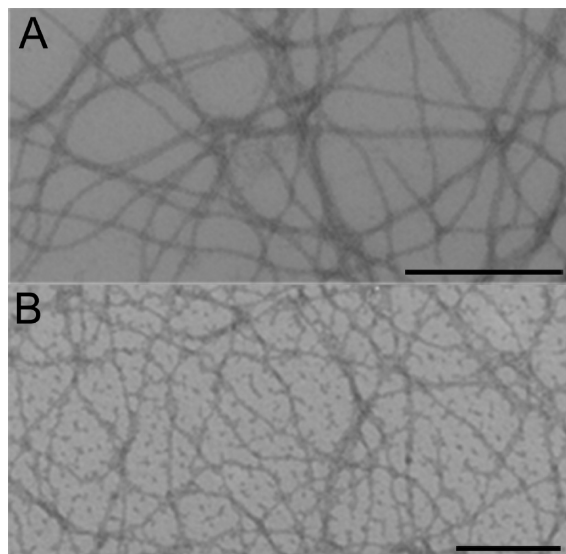


Figure 5. TEM images of aqueous suspensions of Me₂PE-C32-Me₂PE at pH 11 with (A) 100 mM NaCl and (B) 250 mM MgCl₂ at 25 °C. The bar corresponds to 200 nm. The samples were stained with uranyl acetate.

prepared at 25 °C show images with long fibers that are formed after the addition of the salt (Figure 5).

All cations are able to shield the electrostatic repulsion between the negatively charged headgroups and therefore enable a close arrangement of the headgroups in the fiber structure. Considering the similarities between the DSC curves of Me₂PE-C32-Me₂PE at pH 5 and pH 11 with added salts, respectively, and the corresponding TEM images (Figure 5), it is reasonable to assume the same aggregate structure found at pH 5. The presence of fibers above the first transition is also in accordance with the rheological data of these samples (see rheological data below).

In addition, all suspensions with added salt form a gel, with the gelling process being faster for higher salt concentrations and for the divalent cations compared to the monovalent cations. As mentioned above, in the pH value range between 9 and 12 in pure water without additional salt, gelation can only be observed after a few weeks at 4 °C.

In comparing the transition temperatures for the suspensions with NaCl and KCl, it becomes obvious that the stabilizing effect of NaCl on the system is stronger. Several experiments have revealed that monovalent cations have small association constants for binding to negatively charged lipid headgroups and that these constants are higher for sodium than for potassium.^{25,26} The stronger binding of sodium to the negatively charged Me₂PE headgroup compared to potassium is in line with these observations on bilayer systems; it leads to an increased stabilization of the fibers by sodium compared to potassium.

A much lower concentration of the divalent magnesium and calcium cations is necessary to achieve the same stabilizing effect as for the monovalent ions. Compared with the monovalent cations, the association constants are much higher for the divalent cations.^{27,28} In addition, these cations can bind two negatively charged headgroups. A significant difference can also be observed in the gelling process when the solution contains divalent cations. Gelation starts very fast after the addition of the divalent salts at room temperature, whereas for NaCl and KCl

this process may take several days at 4 °C. The divalent cations can not only bind two adjacent headgroups in the same fiber but can also enhance the cross-linking of the fibers by connecting two fiber strands leading to the formation of stronger gels (see rheological data below).

Calcium has a greater stabilizing effect on the fiber and gel structure than magnesium. The main reason is to be seen in the stronger binding of the calcium cations to the headgroups containing negatively charged phosphate groups through the formation of inner sphere complexes as shown by calorimetric measurements with DMPG²⁹ and in other works concerning the interaction between lipids and divalent cations.^{27,30} This apparently leads to increased stability of the fiber and the gel structure compared to the measurements with magnesium.

The appearance of only two transitions at higher concentration of MgCl₂ can be explained if the heating curves of the suspensions containing 100 mM and 250 mM MgCl₂ with heating rates of 60 °C h⁻¹ are compared (Figure 4C, dotted curves). These curves exhibit a split second transition compared to a single transition observed with heating rates of 20 °C h⁻¹. At 1 mM MgCl₂, three transitions are observed, regardless of the heating rate. The fiber–micelle transition (second transition) is shifted by 3 °C to higher temperatures, and the micelle–micelle transition is shifted to lower temperatures by 10 °C in contrast to the suspension in acetate buffer. At a concentration of 100 mM MgCl₂ the temperature difference between both transitions is so small that they superimpose into one and can only be resolved when the heating rate is increased. This transition then combines the transformation of the fiber structure into micelles and the micelle–micelle transition, where an increase in fluidity of the alkyl chains inside the micelles takes place. This is also supported by the transition enthalpy of the merged transition, which has about the same value as the sum of the fiber–micelle and micelle–micelle transitions (Table 2).

For 100 mM CaCl₂ the DSC cooling curves also show the splitting of the transition that was already observed for MgCl₂ (data not shown).

Rheology of Me₂PE-C32-Me₂PE. In aqueous suspensions of Me₂PE-C32-Me₂PE the bolalipids form a transparent gel consisting of a dense three-dimensional network of nanofibers. This gel can be influenced depending on the pH value and the salt concentration. To investigate the gel properties such as strength and viscoelasticity, we used oscillatory rheology. The storage modulus G' is a measure of the elastic properties of the viscoelastic gel, whereas the loss modulus G'' represents the viscous behavior. The rheological behavior of Me₂PE-C32-Me₂PE at pH 5 was studied before¹⁹ and was repeated here for purposes of comparison when the influence of the salt concentration at pH 11 on the rheological behavior was studied. In addition, a higher density of measuring points and a wider temperature range could be realized to investigate the changes in G' and G'' more closely.

The rheological measurements were made under the same conditions as the DSC measurements to ensure comparability. Deformation ($\gamma = 1\%$) and angular frequency ($\omega = 1 \text{ rad s}^{-1}$) were chosen inside the linear viscoelastic region (Figure 6).

The amplitude sweep in Figure 6A shows that G' and G'' are independent of the deformation up to approximately 30%. At higher deformations strain stiffening is observed followed by the crossover of G' and G'' indicating the transition from gel to sol. The frequency sweep at 2 °C shows a plateau of G' up to 10 rad s⁻¹ (Figure 6B) at the concentration $c = 1 \text{ mg mL}^{-1}$. G'' increases with

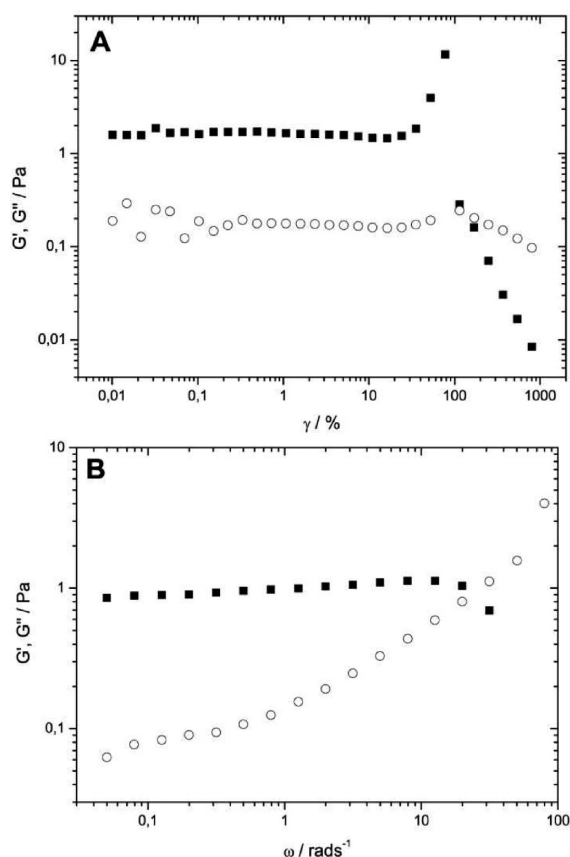


Figure 6. (A) Amplitude sweep (with $\omega = 1 \text{ rad s}^{-1}$) and (B) frequency sweep (with $\gamma = 1\%$) of a suspension of Me₂PE-C32-Me₂PE ($c = 1 \text{ mg mL}^{-1}$) in buffer at pH 5 at 2 °C. G' , filled squares; G'' , open circles.

increasing angular frequency until a crossover at 20 rad s^{-1} occurs. This behavior is caused by the high angular frequency and probably wall slip at the interface of cone and gap with the sample.

Figure 7 displays G' and G'' as a function of temperature together with the calorimetric data of a suspension of Me₂PE-C32-Me₂PE in acetate buffer at pH 5. Up to approximately 45 °C G' is about 1 order of magnitude larger than G'' . Both moduli are quite independent of temperature in this region. Correlating with the fiber–fiber transition, we can observe a large drop in G' and G'' at 45 °C. Above this temperature the difference in G' and G'' decreases; however, G' is still larger. Only at approximately 60 °C, which is slightly below the fiber–micelle transition of the aggregates, G' and G'' have about the same magnitude. At these temperatures the moduli are close to the limit of the measuring range of the rheometer and show a quite large scattering of data as the suspension becomes very fluid.

Below 45 °C G' and G'' show the characteristic behavior of a gel with viscoelastic properties. These data support the macroscopic observation of the gelation. At 45 °C the macroscopic breakdown of the gel can be observed but the fiber structure and a weak viscoelasticity remain intact as was previously shown with rheology, cryo-TEM, and SANS measurements.^{15,19} At this temperature the cross-linking between the hydrophobic parts of different fiber strands via hydrophobic interactions, the hydrogen bonding between the headgroups, and the entanglement of fibers weaken.^{15,19} During the fiber–micelle transition at 68 °C the fiber structure breaks down and the molecules

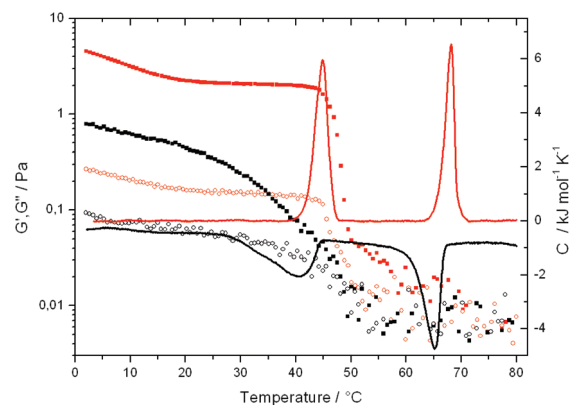


Figure 7. DSC curves (solid lines) and rheological data (G' , filled squares; G'' , open circles) of an aqueous suspension of Me₂PE-C32-Me₂PE in buffer at pH 5 ($c = 1 \text{ mg mL}^{-1}$). Heating, red; cooling, black. The heating and cooling rate was 20 °C h^{-1} . Deformation ($\gamma = 1\%$) and angular frequency ($\omega = 1 \text{ rad s}^{-1}$) were chosen inside the linear viscoelastic region.

self-assemble into spherical micelles. This micellar solution exhibits no viscoelastic properties and shows Newtonian behavior. These results are in accordance with the previous measurement¹⁹ showing a nearly 10-fold decrease in G' due to the almost 10-fold lower concentration. In the temperature range from 2 to 20 °C a steady decrease in G' occurs followed by constant values up to 45 °C. Upon cooling, G' and G'' show a hysteresis and the re-formation of the gel structure does not occur until the sample is cooled to 50 °C. Subsequently a slow increase can be monitored, but the initial values of G' and G'' are reached only after tempering several hours at 2 °C (Figure S2 in the Supporting Information).

The results of the rheological measurements with Me₂PE-C32-Me₂PE at pH 11 for some concentrations of NaCl, KCl, MgCl₂, and CaCl₂ are shown in Figure 8. The values for deformation ($\gamma = 1\%$) and angular frequency ($\omega = 1 \text{ rad s}^{-1}$) inside the linear viscoelastic region could be chosen identically to the measurements at pH 5 due to the very similar amplitude and frequency sweeps of the samples (Figure S3 in the Supporting Information).

For the monovalent cations sodium and potassium (Figure 8A,B) the data show the characteristics of weak viscoelastic gels with G' being larger than G'' and independent of temperature up to the transition at 45 °C. This correlates well with the DSC transition temperatures of the fiber–fiber transition (Table 1). Above this temperature a fast decrease in G' and G'' can be observed. At lower concentrations of NaCl the gel–sol transition (G'' equal to G') occurs right after this decrease, indicating the loss of the gel character. With increasing concentrations this transition is shifted to higher temperature, resulting in gels that are stable up to 55 °C. The same effects can be observed when KCl is added, but they are a little less pronounced. The re-forming of the gel structure after cooling is also affected by the salt concentration and is becoming faster with increasing amount of salt (Figure S4 in the Supporting Information). For the monovalent cations, the values of G' and G'' do not depend on the salt concentration.

If divalent cations are used instead, it is obvious that the moduli are larger even at smaller concentrations, emphasizing the stronger effect on the stabilization of the fiber structure

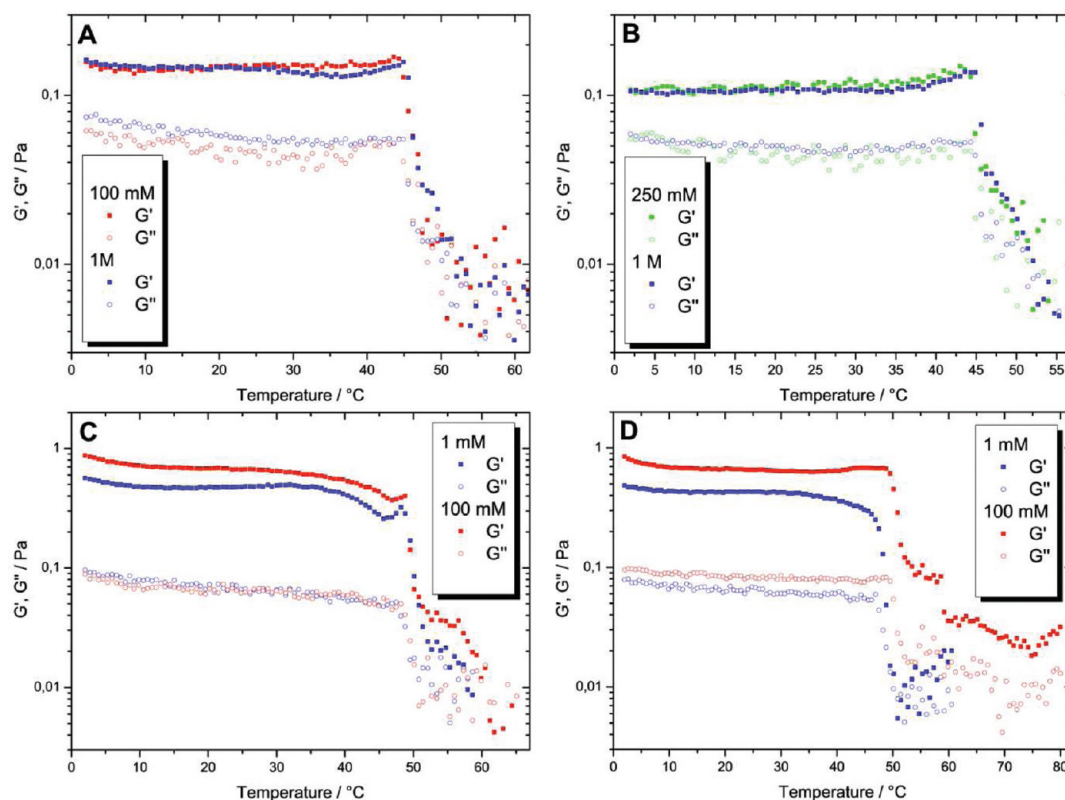


Figure 8. Temperature dependent rheological data of Me₂PE-C32-Me₂PE suspensions ($c = 1 \text{ mg mL}^{-1}$) at pH 11 with (A) NaCl, (B) KCl, (C) MgCl₂, and (D) CaCl₂ at selected concentrations (G' , filled squares; G'' , open circles). The heating rate was $20 \text{ }^{\circ}\text{C h}^{-1}$. Deformation ($\gamma = 1\%$) and angular frequency ($\omega = 1 \text{ rad s}^{-1}$) were chosen inside the linear viscoelastic region.

induced by calcium and magnesium (Figure 8C,D). The changes in G' and G'' follow the same pattern as for the sodium and potassium cations, and the transition temperatures correspond well with those determined from the DSC data (Table 2). Even at 1 mM MgCl₂ the gel stays stable up to $52 \text{ }^{\circ}\text{C}$ and the stability range extends up to $60 \text{ }^{\circ}\text{C}$ at 100 mM MgCl₂, which is just a little below the second transition, supporting the interpretation of this transition as the conversion of fibers into micelles. In the case of 100 mM CaCl₂ this effect is even more evident as G' remains larger than G'' over the whole temperature range. The second distinct step in the decrease of G' correlates with the onset of the rather broad DSC transition temperature. The stability of the gel structure even above this second DSC transition might be due to a slow breaking up of the fibers into micelles during this transition that would take more time to be fully completed at this salt concentration.

The rheological data with 100 mM MgCl₂ and CaCl₂ show a second plateau of G' above the fiber–fiber transition at which G' has about the same value as for all concentrations of NaCl and KCl (Figure 8C,D). This suggests a kind of intermediate state in the gel stability that is formed if the formation of the gel structure is disturbed, e.g., by insufficient shielding of the negative charge in the case of monovalent ions or higher temperatures in the case of bivalent cations.

The values for G' are much higher for Me₂PE-C32-Me₂PE in buffer at pH 5 than at pH 11 with monovalent or divalent cations (4.5 Pa compared to 0.15 Pa and around 0.7 Pa, respectively); nevertheless it is obvious that the salts are able to transform the viscous behavior of Me₂PE-C32-Me₂PE suspensions at pH 11 into the behavior of a viscoelastic gel. For the divalent cations the

moduli, in contrast to the monovalent ions, increase with increasing salt concentration.

As was shown by DSC and TEM investigations, the fibers can, at basic pH values, be re-formed in the presence of the salts, but the shielding of the negatively charged headgroups and the cross-links between the fibers are still too weak to retain the viscoelastic gel properties above the fiber–fiber transition, at least at small salt concentrations. With increasing salt concentration the gels are stable up to higher temperatures, and at the highest concentrations they are stable up to the onset of the fiber–micelle transition. Above this temperature G' and G'' become very small and the behavior can be described as that of a Newtonian fluid, as described for Me₂PE-C32-Me₂PE suspensions above pH 10.¹⁹

The rheological analysis of the Me₂PE-C32-Me₂PE gels reveals a behavior that differs distinctly from the behavior of gels formed by wormlike micelles. A very common property of these gels is their Maxwell behavior with a single relaxation time.^{6,9,31} The relaxation time is linked to the breaking time and the reptation time of the wormlike micelles. In the fast breaking limit the micelles undergo several breaking and recombination reactions in the time scale of the reptation.^{9,32} In the frequency spectra this Maxwellian behavior can be monitored in the crossover of G' and G'' at low frequency. However, at $2 \text{ }^{\circ}\text{C}$ this cannot be observed in the frequency spectra of gels of Me₂PE-C32-Me₂PE at pH 5 or at pH 11 in the presence of higher amounts of salts (Figure 6 and Figure S3 in the Supporting Information). An increase of the gel strength with the concentration of the bolaamphiphile in suspension also enables the measurement of frequency spectra of a Me₂PE-C32-Me₂PE suspension ($c = 8 \text{ mg mL}^{-1}$) at elevated temperatures. These measurements show

that even at 55 °C no crossover can be monitored at low frequencies (Figure S5 in the Supporting Information).

The absence of a crossover of G' and G'' at low frequencies indicates a very long relaxation time and the behavior of an elastic gel as was also described for EDAB (erucyl dimethyl amidopropyl betaine) samples at low temperatures.^{8,33} However, the G' and G'' values for gels from Me₂PE-C32-Me₂PE are more than 100-fold higher at the same concentration, showing the high efficiency of gelation of the fibers formed from bolalipids.

The independence of G' and G'' from frequency over a certain range is common for all gels, but gels of wormlike micelles also show high straining limits in contrast to gels of crystalline nanofibers that have straining limits as low as 2%.⁴ The bolaamphiphile gels are only disrupted if the deformation gets higher than about 100% and they also exhibit strain stiffening right before an abrupt decrease in G' and G'' (Figure 6 and Figure S3 in the Supporting Information). This phenomenon has been reported for organogels⁵ and is also common in biological materials, such as collagen, fibrin, or actin networks.³⁴ This shows again the intermediate behavior of gels formed by the stiff bolalipid nanofibers.

The recovery of the gel structure of Me₂PE-C32-Me₂PE may take several hours and depends on concentration. This is due to the fact that the fibers have to be formed from single dispersed micelles. The nature of the nucleation process is not known at the moment. In addition, a relatively well ordered alignment of the all-*trans* alkyl chains inside the aggregates has to occur. Therefore, the nanofibers formed by Me₂PE-C32-Me₂PE have a larger similarity to the high order in crystalline nanofibers. This is also the reason for the disagreement with the Maxwell model used for wormlike micelles, as the scission and recombination of these fibers with higher chain order takes more time than for the wormlike micelles.

CONCLUSION

The single-chain symmetrical bolaamphiphile Me₂PE-C32-Me₂PE self-assembles into fibers in aqueous suspensions depending on the pH value and the salinity. At pH values higher than 10 the negatively charged headgroups impede the aggregation into fibers and the stability range is shifted to lower temperatures. The ability of the Me₂PE-C32-Me₂PE fibers to gel the suspension is dependent on the pH value, decreasing with an increasing amount of charged headgroups. The formation of fibrous aggregates can be enhanced by the addition of cations that shield the repulsive forces between the headgroups inside the aggregates. Divalent cations such as calcium and magnesium have been shown to have a stronger stabilizing effect than the monovalent ions sodium and potassium due to the higher binding constants.

The rheological properties of Me₂PE-C32-Me₂PE suspensions vary from the behavior of a viscoelastic gel at pH 5 to that of a Newtonian fluid at pH 10 and higher pH values. The addition of salts at pH 11 results in the re-formation of the viscoelastic gel properties. The influence of the cations on the rheological behavior exhibits the same tendencies as on the thermal stability as observed by DSC measurements. If the salinity is high enough, the viscoelastic gel structure is stable up to the fiber–micelle transition.

Although the fibers and gel structure described for Me₂PE-C32-Me₂PE reveal several properties that are similar to the ones described for wormlike micelles (e.g., transparent gel, high

straining limit, and a slope of -1 in the scattering data), the frequency spectra of the suspensions show a behavior that is uncommon in gels of wormlike micelles. Due to the high degree of order (all-*trans* alkyl chains) inside the fibers, slower breaking and re-forming reactions than in the case of wormlike micelles are observed. The bolalipid gels show more similarity to the rheological behavior of biological materials, such as collagen or actin and fibrin fiber networks. The bolalipid suspensions can be switched between gel behavior and Newtonian fluid by changing the temperature, the pH value, or the salt concentration at high pH. However, due to slow nucleation and growth from micellar structures, the re-formation of the gel is dependent on the bolalipid concentration and may take several hours at low bolalipid concentration.

ASSOCIATED CONTENT

S Supporting Information. DLS measurements and rheological data. This information is available free of charge via the Internet at <http://pubs.acs.org>.

AUTHOR INFORMATION

Corresponding Author

*Tel.: +49-345-5525850. Fax: +49-345-5527157. E-mail: alfred.blume@chemie.uni-halle.de.

ACKNOWLEDGMENT

We thank the Deutsche Forschungsgemeinschaft (Projects Bl 182/19-3 and Do 463/4-2) for financial support. The support of Gerd Hause (Biocenter, Martin-Luther-University Halle-Wittenberg) by providing us access to the electron microscope facility is greatly appreciated. Finally, we thank Sebastian Zimmermann for the data of his first rheological measurements on hydrogels.

REFERENCES

- (1) Terech, P.; Weiss, R. G. *Chem. Rev.* **1997**, *97*, 3133–3160.
- (2) Estroff, L. A.; Hamilton, A. D. *Chem. Rev.* **2004**, *104*, 1201–1218.
- (3) Sangeetha, N. M.; Maitra, U. *Chem. Soc. Rev.* **2005**, *34*, 821–836.
- (4) Raghavan, S. R. *Langmuir* **2009**, *25*, 8382–8385.
- (5) Tung, S.-H.; Huang, Y.-E.; Raghavan, S. R. *Soft Matter* **2008**, *4*, 1086–1093.
- (6) Tung, S.-H.; Huang, Y.-E.; Raghavan, S. R. *Langmuir* **2007**, *23*, 372–376.
- (7) Wang, T.; Jiang, J.; Liu, Y.; Li, Z.; Liu, M. *Langmuir* **2010**, *26*, 18694–18700.
- (8) Kumar, R.; Kalur, G. C.; Ziserman, L.; Danino, D.; Raghavan, S. R. *Langmuir* **2007**, *23*, 12849–12856.
- (9) Dreiss, C. A. *Soft Matter* **2007**, *3*, 956–970.
- (10) Fuhrhop, J.-H.; Wang, T. *Chem. Rev.* **2004**, *104*, 2901–2937.
- (11) Meister, A.; Blume, A. *Curr. Opin. Colloid Interface Sci.* **2007**, *12*, 138–147.
- (12) Meister, A.; Drescher, S.; Garamus, V. M.; Karlsson, G.; Graf, G.; Dobner, B.; Blume, A. *Langmuir* **2008**, *24*, 6238–6246.
- (13) Drescher, S.; Meister, A.; Blume, A.; Karlsson, G.; Almgren, M.; Dobner, B. *Chem.—Eur. J.* **2007**, *13*, 5300–5307.
- (14) Koehler, K.; Foerster, G.; Hauser, A.; Dobner, B.; Heiser, U. F.; Ziethe, F.; Richter, W.; Steiniger, F.; Drechsler, M.; Stettin, H.; Blume, A. *J. Am. Chem. Soc.* **2004**, *126*, 16804–16813.
- (15) Koehler, K.; Meister, A.; Foerster, G.; Dobner, B.; Drescher, S.; Ziethe, F.; Richter, W.; Steiniger, F.; Drechsler, M.; Hause, G.; Blume, A. *Soft Matter* **2006**, *2*, 77–86.

- (16) Meister, A.; Drescher, S.; Karlsson, G.; Hause, G.; Baumeister, U.; Hempel, G.; Garamus, V. M.; Dobner, B.; Blume, A. *Soft Matter* **2010**, 6, 1317–1324.
- (17) Drescher, S.; Graf, G.; Hause, G.; Dobner, B.; Meister, A. *Biophys. Chem.* **2010**, 150, 136–143.
- (18) Drescher, S.; Meister, A.; Graf, G.; Hause, G.; Blume, A.; Dobner, B. *Chem.—Eur. J.* **2008**, 14, 6796–6804.
- (19) Meister, A.; Bastrop, M.; Koschoreck, S.; Garamus, V. M.; Sinemus, T.; Hempel, G.; Drescher, S.; Dobner, B.; Richtering, W.; Huber, K.; Blume, A. *Langmuir* **2007**, 23, 7715–7723.
- (20) Candlish, J. K.; Tristram, G. R. *Biochim. Biophys. Acta* **1964**, 88, 553–563.
- (21) Miyoshi, E.; Takaya, T.; Williams, P. A.; Nishinari, K. *Macromol. Symp.* **1997**, 120, 271–280.
- (22) Shoemaker, S. D.; Vanderlick, T. K. *J. Colloid Interface Sci.* **2003**, 266, 314–321.
- (23) Chen, W.-R.; Butler, P. D.; Magid, L. J. *Langmuir* **2006**, 22, 6539–6548.
- (24) Meister, A.; Drescher, S.; Mey, I.; Wahab, M.; Graf, G.; Garamus, V. M.; Hause, G.; Mogel, H. J.; Janshoff, A.; Dobner, B.; Blume, A. *J. Phys. Chem. B* **2008**, 112, 4506–4511.
- (25) Seantier, B.; Kasemo, B. *Langmuir* **2009**, 25, 5767–5772.
- (26) Ermakov, Y. A. *Biochim. Biophys. Acta, Biomembr.* **1990**, 1023, 91–97.
- (27) Marra, J.; Israelachvili, J. *Biochemistry* **1985**, 24, 4608–4618.
- (28) Böckmann, R. A.; Hac, A.; Heimbürg, T.; Grubmüller, H. *Biophys. J.* **2003**, 85, 1647–1655.
- (29) Garidel, P.; Blume, A. *Langmuir* **1999**, 15, 5526–5534.
- (30) Tatulian, S. A. *Eur. J. Biochem.* **1987**, 170, 413–420.
- (31) Kumar, R.; Raghavan, S. R. *Soft Matter* **2009**, 5, 797–803.
- (32) Berret, J. F. In *Molecular Gels. Materials with Self-Assembled Fibrillar Networks*; Weiss, R. G., Terech, R., Eds.; Springer: Dordrecht, The Netherlands, 2006.
- (33) Larson, R. G. *The Structure and Rheology of Complex Fluids*; Oxford University Press, Inc.: New York, 1999.
- (34) Storm, C.; Pastore, J. J.; MacKintosh, F. C.; Lubensky, T. C.; Janmey, P. A. *Nature* **2005**, 435, 191–194.